ELSEVIER

Journal of Nuclear Materials 299 (2001) 1–8

journal of nuclear materials

www.elsevier.com/locate/jnucmat

Analysis of singular interface stresses in dissimilar material joints for plasma facing components

J.H. You *, H. Bolt

Max-Planck-Institut für Plasmaphysik, EURATOM Association, Boltzmannstr. 2, D-85748 Garching, Germany

Received 13 June 2001; accepted 15 August 2001

Abstract

Duplex joint structures are typical material combinations for the actively cooled plasma facing components of fusion devices. The structural integrity under the incident heat loads from the plasma is one of the most crucial issues in the technology of these components. The most critical domain in a duplex joint component is the free surface edge of the bond interface between heterogeneous materials. This is due to the fact that the thermal stress usually shows a singular intensification in this region. If the plasma facing armour tile consists of a brittle material, the existence of the stress singularity can be a direct cause of failure. The present work introduces a comprehensive analytical tool to estimate the impact of the stress singularity for duplex PFC design and quantifies the relative stress intensification in various materials joints by use of a model formulated by Munz and Yang. Several candidate material combinations of plasma facing armour and metallic heat sink are analysed and the results are compared with each other.

1. Introduction

1.1. Thermal stresses in plasma facing components

Future fusion devices will be equipped with actively cooled plasma facing components (PFCs) to transfer the surface heat flux incident onto the plasma facing material (PFMs) via a heat sink to the coolant. Duplex joint structures are usually applied for these components. Typically, this duplex joint structure consists of plasma facing armour tiles which are bonded to a metallic heat sink substrate. The heat sink substrate is furnished with coolant channels. Thus, the incident heat flux will be conducted through the PFM tile and the bond interface into the heat sink substrate.

The high heat flux (HHF) generates thermal stresses in the PFCs. An important source of these thermal stresses is the difference in the coefficient of thermal expansion (CTE) of the constituting materials. This causes the so-called mismatch stress especially in the region near the bond interface between PFM armour tile and heat sink substrate [1,2]. The contribution from the mismatch stress to the total thermal stress can be essential.

The mismatch thermal stress is controlled mainly by the change of temperature at the bond interface, provided that steep thermal gradients are not the cause of any further significant stress contribution [3,4]. Such a mismatch stress can be generated already during the manufacturing process of joints resulting in residual stresses within the component [5,6]. The additional stress from the subsequent thermal loading will be superposed on this residual stress field. Under this circumstance, the temperature difference between the stress free state and the current state is the controlling parameter.

1.2. Motivation

The structural integrity is one of the most crucial issues in the PFC technology. The selection of the proper material combination, an optimised component design and the estimation of the load limit are the main factors of design considerations. The interplay of the

* Corresponding author. Tel.: +49-89-3299-1373; fax: +49-89-3299-1212.

E-mail address: jeong-ha.you@ipp.mpg.de (J.H. You).

0022-3115/01/$ - see front matter
PII: S0022-3115(01)00680-8

thermal stress in the components and the resistance of the candidate materials against mechanical failure is an essential concern. From the viewpoint of structural integrity, the most critical domain in a duplex joint component is the free surface edge of the bond interface. This is due to the fact that the thermal stress distribution usually shows an intense peak in this region. This is known as the stress singularity and has been characterised extensively [7–10]. The singular fields can generate a significant intensification of stresses compared to the stress occurring at the interface distant from a free surface. If the plasma facing armour tile is made of a brittle material, the existence of stress singularities can be a direct cause of failure. Interfacial debonding or fracture of armour tiles is the main failure mode. This behaviour has been observed in many component tests [2].

To assess the impact of the stress singularity problem on the design of PFCs, a rigorous analytical description for the singular stress fields is necessary, since it shows the correlation between the loading parameters and the material properties directly. A comparative analysis for various material combinations will give the data on the relative performance of these duplex structures. The purpose of this work is: (i) to introduce a comprehensive analytical tool to estimate the impact of the stress singularity for duplex PFC design and (ii) to quantify the relative stress intensification in various material joints.

In this work, a theoretical model is applied which was formulated by Munz and Yang [9]. Using this model, the role of constituting parameters is investigated. A possible design parameter describing the intensity of a singular stress field is introduced from literature. The validity of the present model for the HHF loading situation is also discussed. Several candidate material combinations of PFM and metallic heat sink are analysed and the results are compared.

The exact computation of stress fields needs, of course, the consideration of details of the component geometry. In addition, the temperature dependence of material properties should be taken into account. However, these features are neglected in this work, since the complicated boundary conditions and the temperature dependent properties can hardly be handled in a fully analytical framework. However, a simplified analytical estimation can provide us with comprehensive insight into the structural integrity behaviour of PFCs. It could be applied to the materials screening procedure prior to a detailed structural design based on numerical methods.

2. Theory

2.1. Model geometry and basic concept

The geometry of the duplex material structure used for the present analysis is shown in Fig. 1. For the sake of simplicity, the boundary conditions and the load case were simplified without loosing the essential feature of the loading characteristics for plasma facing components of fusion reactors.

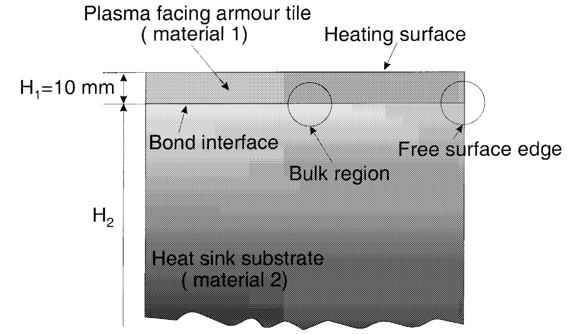

Fig. 1. Schematic of a duplex bond joint for a plasma facing component.

The thickness of the armour tile and substrate used for this analysis is 10 and 100 mm, respectively, (see Fig. 1). The PFM thickness of 10 mm has been considered as a typical dimension of plasma facing armour tiles for next step devices [6]. The substrate thickness of 100 mm is chosen somewhat arbitrarily taking into account the large moment of inertia of a first wall directly joined to the blanket or to the backing structure. A rectangular edge geometry is considered. The contact angles of the bond interface cutting the free surface edge are 90°.

The thermal stress in the bulk region of a bi-material joint under uniform temperature change can be completely described using the classic beam theory [1]. One of the basic premises of such models is that the vertical planar cross section remains planar after bending, which is known as the Bernoulli assumption. However, in the region near the free surface edge of the bond interface, the Bernoulli assumption will break down due to the free boundary effect and since the deformation field is no longer uniaxial. In case the elastic misfit is large enough, the local surface deformation near the interface can be severe and the stress field shows sometimes a singularity. For a brittle PFM, this stress intensification can lead to undesirable dynamic fracture. In numerous HHF experiments conducted on PFC modules, it has been observed that the free surface edge of the bond interface was the most probable site of crack initiation. Therefore, the analysis of the singular stress field can be a critical factor in design considerations for PFCs.

In the following section, one analytical model for such a treatment is shortly explained. Emphasis is placed on the formulation of a model which incorporates the underlying parameters describing the singular stress field.

2.2. Description of singular stress fields

Based on the analogy of linear elastic fracture mechanics, Munz and Yang suggested that the singular stress field can be described by

$$\sigma_{ij}(r,\theta) = \frac{K}{(r/D)^{\omega}} f_{ij}(\theta) + \sigma_0 f_{ij0}(\theta), \tag{1}$$

for a rectangular wedge geometry (contact angles are 90°) [9]. The position r (distance from free surface) is normalised by a characteristic dimension D of the joint. It can be either the thickness H_1 (or H_2) or the half of the width L. The corresponding geometry for this model is shown in Fig. 2. The parameters ω, $f_{ij}(\theta)$, K and σ_0 are dependent on the elastic modulus E and the Poisson ratio ν. In addition, the stress intensity factor K and the regular stress term σ_0 are proportional to the mismatch of CTEs, α, and the temperature difference ΔT. For mechanical loading, σ_0 is zero. The exponent of singularity ω, the angular functions f_{ij} and the regular stress term σ_0 can be determined analytically.

According to Bogy, the singularity exponent ω can be obtained by solving the following characteristic equation [7,11]:

$$\lambda^2(\lambda^2-1)\alpha^2 + 2\lambda^2\left[\sin^2(\pi\lambda/2)-\lambda^2\right]\alpha\beta + \left[\sin^2(\pi\lambda/2)-\lambda^2\right]^2\beta^2 + \sin^2(\pi\lambda/2)\cos^2(\pi\lambda/2) = 0, \tag{2}$$

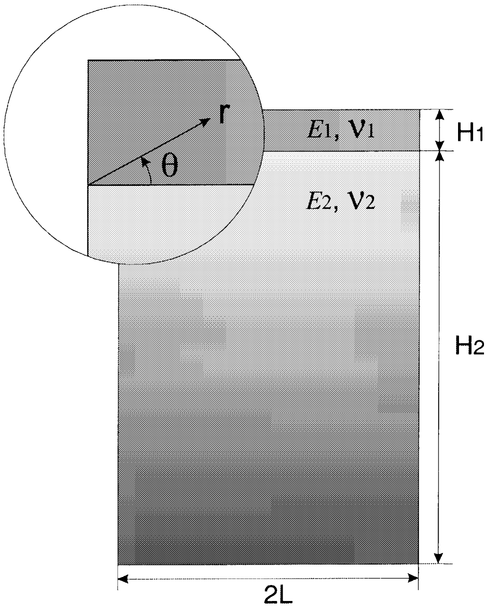

Fig. 2. Geometry of the joint model used for the present analysis.

where

$$Re(\lambda) = 1-\omega, \tag{3}$$

$$\alpha = \frac{m_2 - km_1}{m_2 + km_1}, \tag{4a}$$

$$\beta = \frac{(m_2-2)-k(m_1-2)}{m_2+km_1}, \tag{4b}$$

with

$$k = \mu_2/\mu_1, \tag{5a}$$

$$m_i = 4(1-\nu_i) \quad \text{(plane strain)}. \tag{5b}$$

The elastic constant μ_i denotes the shear modulus of material i. This equation was derived under the condition that the linear system of solution equations for the boundary value problem of the stress singularity should have a non-trivial solution set for displacements and stresses. It has to be noted that the roots of Eq. (2) depend only on Dundurs' parameters α and β, i.e., on elastic constants.

The components of the second angular function are

$$f_{rr0} = \tfrac{1}{2}(1-\cos 2\theta), \tag{6a}$$

$$f_{\theta\theta 0} = \tfrac{1}{2}(1+\cos 2\theta), \tag{6b}$$

$$f_{r\theta 0} = \tfrac{1}{2}\sin 2\theta \tag{6c}$$

and the regular stress term σ_0 is

$$\sigma_0 = \Delta\alpha^{*}\Delta E^{*}\Delta T, \tag{7}$$

with

$$\Delta\alpha = \alpha_1(1+\nu_1) - \alpha_2(1+\nu_2) \quad \text{(plane strain)}, \tag{8a}$$

$$\Delta E^{*} = \left[\frac{1}{E_1^{*}} - \frac{1}{E_2^{*}}\right]^{-1}, \tag{8b}$$

$$E_i^{*} = \frac{E_i}{\nu_i(1+\nu_i)} \quad \text{(plane strain)}. \tag{8c}$$

Formulas for the angular functions f_{ij} are omitted, as they are too complicated to be given here. They can be found in the literature of Munz and Yang [12].

K is the parameter which includes the effect of the external load (e.g., temperature change) and the far field boundary conditions. In principle, it has to be obtained from a finite element analysis. But it can also be obtained analytically for the specific range of the thickness ratios [9,12]. The stress intensity factor K can be considered as a useful measure of the stress intensification near the singular point, although its physical dimension differs from that of the classical fracture mechanics. The effect of the joint geometry as well as the loading history on the stress concentration can be clearly assessed by investigating the behaviour of K for a given material combination. It should be noted that the K-factor is not influenced by the component size itself, whereas the singular stress is significantly size dependent by the factor D^{ω}.

By controlling the K, σ_0 and ω values, the strength of singular stress fields can be minimised. For instance, there exists a range of Dundurs' parameters for which the stress singularity completely vanishes. This can be achieved by choosing a material combination which has a minute difference in effective elastic moduli [9],

$$\frac{E_1^* - E_2^*}{E_1^* + E_2^*} \leqslant 0.2. \tag{9}$$

However, the tendency of dependence of K and ω on $E_1^* - E_2^*$ is inconsistent with each other so that the resultant stress does not vary monotonically with the change of ω (or $E_1^* - E_2^*$). Thus, the optimal combination can be found not by a simple consideration of the trend of interrelations of individual parameters but only by full computation of the singular stress using Eq. (1). Despite of the complexity stated above, it can be still thought that σ_0, ω and K can be useful design parameters for the selection of proper materials for PFCs, since σ_0 and ω depend exclusively on the material constants and ΔT, whereas K includes the effect of load and boundary condition.

2.3. Average singular stress

A quantity $\bar{S}_{ij}$ which is defined as an averaged singular stress in the near field of free surfaces was introduced by Kroupa et al. to represent the strength of a stress singularity [13]. This average singular stress is written as

$$\bar{S}_{ij} = \frac{1}{r_0/D}\int_0^{r_0/D} \sigma_{ij}(r)\big|_{\theta_0} d(r/D) = \frac{K f_{ij}}{(1-\omega)(r_0/D)^{\omega}} + \sigma_0 f_{ij0}, \tag{10}$$

where r_0 is the extent of averaging operation in radial direction.

The average singular stress $\bar{S}_{ij}$ is a combination of the three parameters, σ_0, ω and K. Though it seems to be not so simple, it provides a quantitative measure for the strength of the singular stress field with a clear physical meaning. The sign of stress in the singular field is still maintained in $\bar{S}_{ij}$ but caution has to be given when the stress sign changes within the integration interval.

2.4. Effect of non-linear temperature profile

This model was originally developed for uniform temperature distribution. Later it was extended to non-uniform temperature profiles by introducing additional terms coupled with temperature gradients [14].

In case of HHF loading, it was shown that both ω and K are just weakly influenced by the non-linear temperature profile, if the assumed HHF load remains within the range of normal operation condition (ca. 20 MW/m^2) [15]. This indicates that the analytical method for a uniform temperature field can still be used for a HHF loading case without further modification.

3. Materials

In this work, nine material combinations consisting of three different plasma facing materials for the armour tile and three structural materials for the heat sink substrate are examined. Materials considered are graphite (EK98), CFC (Sepcarb N112) and tungsten (stress relieved grade) as PFMs (i.e. armour tiles) and copper alloy (CuCrZr), martensitic–ferritic steel (9Cr1Mo) and vanadium alloy (V4Cr4Ti) as heat sink substrates.

For a straightforward analysis, all materials listed above are assumed to remain in the elastic regime under the applied heat load. This assumption may be reasonable, when the equivalent stress of the metallic materials remains within the yield limit. If the equivalent stress exceeds the yield stress, the elastic solution will overestimate the real stress. In addition, the temperature dependence of the material properties is neglected. The selected material properties are listed in Tables 1 and 2.

4. Results and discussion

The stress concentration in the region near the free surface edge is analysed for the nine material combinations which were already mentioned in Section 3. Only the thermal stresses are considered. For a system of elastic materials, the thermal stresses are determined uniquely by the net temperature change ΔT regardless of the loading path. In case of a bond joint system, ΔT can be defined as the temperature difference at the interface between the stress free-state (e.g., bonding temperature) and the current state. The current state may be either ambient temperature or steady state temperature during the thermal loading. In this work, it is assumed that this current temperature is lower than that of stress-free state. Such a case corresponds to net cooling of the joints from the stress-free temperature to the current temperature directly by a uniform temperature change. After having determined the three constituting parameters, the resulting singular stress field is calculated.

Before we discuss the results, it should be noted that the stress intensity factor K in Eq. (1) is a single scalar value. This means that the stress intensity factor is the common parameter for all stress components in the singular fields of the perfectly bonded interface. In contrast to this, the singular stress fields in front of an interfacial crack tip have to be characterised by a

Table 1
Selected properties of the plasma facing materials [16–18]

	Graphite (EK 98)	CFC[a] (N112)	Tungsten
Coefficient of thermal expansion[b] (K^{-1})	5.2×10^{-6}	1.5×10^{-6}	4.1×10^{-6}
Young's modulus (GPa)[b]	10	28	395
Poisson's ratio[b]	0.18	0.11	0.28
Yield stress (MPa) (20 °C)	–	–	1360
(300 °C)	–	–	1050
(600 °C)	–	–	760

[a] In-plane direction.
[b] Data at 300 °C.

Table 2
Selected properties of the substrate materials [18,19]

	Copper alloy (CuCrZr)	Steel 9Cr1Mo	V alloy (V4Cr4Ti)
Coefficient of thermal expansion[a] (K^{-1})	17.6×10^{-6}	11.5×10^{-6}	10×10^{-6}
Young's modulus (GPa)[a]	115	188	130
Poisson's ratio[a]	0.33	0.3	0.36
Yield stress (MPa) (20 °C)	300	550	390
(300 °C)	250	490	240
(600 °C)	160	280	220

[a] Data at 300 °C.

complex stress intensity factor which has more than one component in the complex space, since the interfacial fracture occurs actually in mixed mode. Each of these components represents the specific crack tip loading mode. To assess the impact of the singular stress fields of an interfacial crack on crack extension, both the normal and the shear stress components should be investigated. The normal stress component is mainly responsible for the mode I fracture (crack opening mode) of the interface, whereas the shear stress component for the mode II fracture (crack sliding mode). The relative portions of each fracture mode contributions depend on the loading condition, materials, interface shape and the position on the interface. The relative portion of the individual fracture modes was investigated in [20] for the carbon-to-molybdenum joint with a similar geometry as in Fig. 2 using the method of the phase angle in the complex space. Assuming that the joint including interfacial cracks was subjected to a typical high heat flux thermal loading, it was shown that the edge crack was loaded purely by the shear mode due to the crack closure phenomenon.

If there is no pre-existing interface crack at the free surface edge, the contribution of the singular shear stress to the crack initiation at the free surface edge is represented by the common stress intensity factor K which also represents the singular normal stress field as well. Hence, these two stress components in the singular fields are proportionally interrelated by K showing the same trend of dependency on K. In this work, only the normal stress component is discussed for simplicity.

The stress components in Figs. 3(a)–(c), normal to the interface plane are plotted. All stress values are normalised by a unit temperature decrease of one degree. The position is also normalised by the thickness of the armour tile. The graphite and the CFC joints show a relatively weak compressive singularity whereas the tungsten joints show a well developed tensile singularity. Since the interfacial fracture is effectively promoted by crack opening loading, the tensile stress intensification can be critical. Therefore, it can be concluded that the joints with tungsten armour tiles (especially, the tungsten–copper joint) experience stronger interfacial loading at free surface edge in comparison to the other joints. This response is due to the high elastic modulus of tungsten and the large difference in CTE values.

However, it should be noted that the amount of local stress itself does not represent the failure likelihood directly, since the fracture criterion requires relative loading strength compared with the toughness of bond interface or armour materials. It is also seen that the normal stress in the CFC–vanadium and CFC–copper joints extends beyond the singular region, whereas the normal stress of other joints is conspicuous only in the singular field and decays rapidly. The CFC–copper joint requires more attention, since considerable tensile normal stress prevails in the intermediate region (between the free surface edge and the bulk region). Interfacial crack extension under repeated thermal cycling can possibly occur due to this tensile normal interface stress.

Actually, the initiation of the edge interface debonding of graphite and CFC tiles will hardly occur

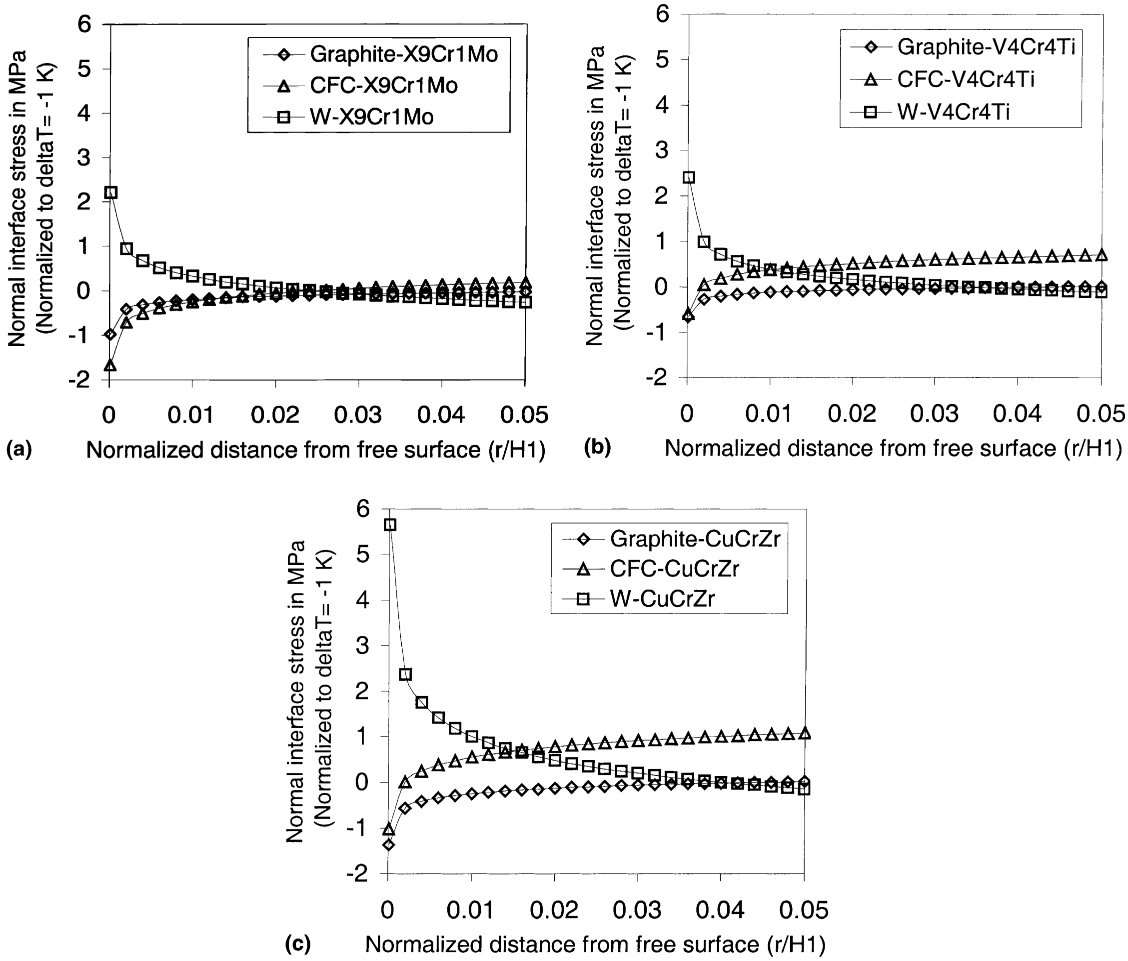

Fig. 3. Distribution of the normal stress component near the free surface edge. Stress values are normalised by a unit temperature decrease of one degree. (a) Joint with steel substrate. (b) Joint with vanadium alloy substrate. (c) Joint with copper alloy substrate.

under monotonous, uniform temperature change, since their singular stress fields are compressive. However, if an interface crack having critical size is nucleated at the edge surface, its growth can be promoted by the sliding mode of crack tip deformation.

According to [12], the sign of the singular stress fields can be uniquely related to four categories each of which represents the specific range of the ratios of the thermo-elastic constants for the joint materials. This relationship is summarised in Fig. 4 in which the ratios of the thermo-elastic constants for three PFMs and for three heat sink materials are also indicated. It is readily confirmed that all the stress results in Fig. 3 satisfy this rule. With help of this diagram, one can easily envisage the sign of singular stress field for a given material combination.

The values of three theoretical parameters K, ω and σ_0 estimated for the material pairs are listed in Table 3. It is important to note that none of these parameters can alone represent the strength of the singular stress fields.

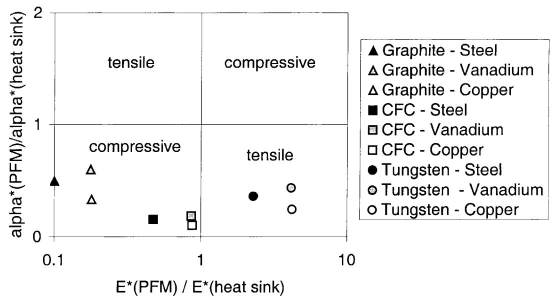

Fig. 4. Rule of sign of the singular interface stress on cooling from stress free state. Data points for the materials combinations used for the analysis are also shown. Stress signs are indicated for the normal stress component of the armour tiles. For each armour tile materials, three data points are assigned which correspond to three heat sink materials, respectively. $\alpha^* = \alpha(1+\nu)$, $E^* = E/\nu(1+\nu)$.

It does not seem to be straightforward to deduce a simple rationale to explain the strength of an individual singular stress field by considering these parameters separately. For example, a specific material combination produces contradicting trends in K and ω, respectively. A combination of these parameters according to Eq. (1) will lead to a singular stress field, which allows no direct correlation to one of these parameters. This feature suggests that any of the theoretical parameters alone would not be a pertinent universal design parameter as far as a comparative estimation of stress singularity for various material combinations is concerned.

One of the reasons for such an intricacy is due to the fact that the spatial extent of influence and its relative strength is different for each parameter, though the parameters have no intrinsic antagonism to each other. Eq. (1) indicates that an increase in each of these parameters will lead to an intensification of the singular stress field to a certain extent (for K, intensification in the same direction of its sign and for σ_0, translation in the same direction of its sign). This behaviour is plotted in Fig. 5 schematically for an arbitrary material joint to show a correlation between the individual parameters and the singular stress field. The effect of σ_0 is omitted here, since it contributes simply by constant addition. It is seen that ω exerts a more sensitive influence than K whereas the working realm of ω is restricted to a much smaller region than that of K.

Comparing with the comprehensive trends in Fig. 5, it is clear again that the results of the stress singularity given in Fig. 3 and the theoretical parameters in Table 3 do not give such a consistent correlation with each other. Hence, the trend regarding the stress singularities of the nine material pairs used cannot be described by a single master parameter. However, if a specific material combination is given, the stress intensity factor K can still be used as a design parameter to characterise the loading nature at the interface edge under varying external load [20,21]. For a large thickness-to-width ratio or vice versa, the variation of K will be nearly proportional to the external load (e.g., temperature change) and stay independent of geometry.

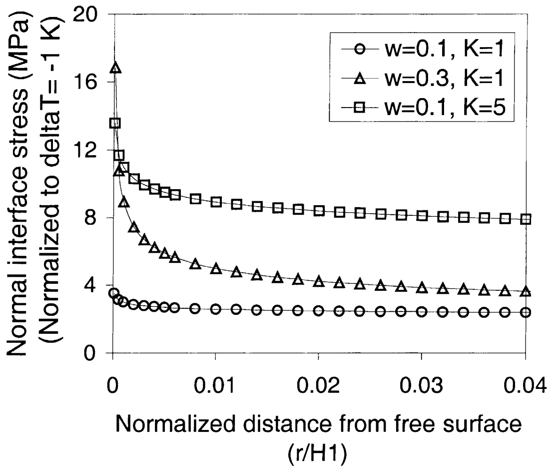

Fig. 5. Influence of theoretical parameters on the strength of the singular stress fields. (Stress values are normalised by a unit negative regular stress term).

The $\bar{S}_{ij}$ values for the nine material joints investigated using Eq. (10) are given in Fig. 6. The results are obtained for $r_0/D = 0.001$. Comparing with the stress distributions in Fig. 3, it is seen that the $\bar{S}_{ij}$ values reflect the actual stress singularity quite consistently. As Munz and Yang already pointed out [12], this quantity can be used as a design parameter to compare the interfacial integrity of different duplex PFCs with various material combinations.

5. Summary

The assessment of thermal stress is an important prerequisite to design a duplex plasma facing component

Table 3
Estimated values of the constituent theoretical parameters for various material combinations. All parameter values are normalised by a unit temperature decrease of one degree Celsius

Joints		Singularity exponent ω	Stress intensity factor K	Regular stress term σ_0
Heat sink	Armour tile			
Copper alloy	Graphite	0.121	−0.85	1.2
	CFC	0.008	−37.9	40
	Tungsten	0.108	4.4	−6.2
Martensitic steel	Graphite	0.15	−0.4	0.6
	CFC	0.046	−4.9	5.8
	Tungsten	0.044	7	−8.2
Vanadium alloy	Graphite	0.127	−0.4	0.6
	CFC	0.011	−18.8	20.1
	Tungsten	0.104	2	−2.9

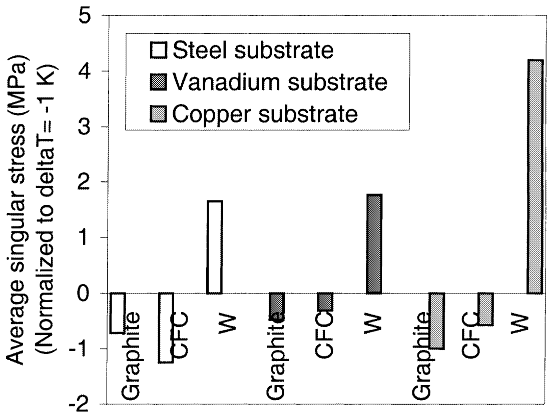

Fig. 6. Average of the normal stress component near the free surface edge for a domain r/H1 of 0.001. Stress values are normalised by a unit temperature decrease of one degree.

which consists of plasma facing armour tiles bonded to a metallic heat sink substrate. In general, the most critical domain in such a duplex joint component is the free surface edge of the bond interface, where a singular stress concentration occurs.

In this article, a fully analytical approach was presented for the treatment of the singular thermal stress field of the duplex plasma facing components. The theoretical model developed by Munz and Yang was applied. Nine material combinations of three plasma facing armour materials and three heat sink metals were investigated.

It was demonstrated that the sign as well as the strength of the singular stress field are essentially influenced by the relative magnitude as well as the degree of mismatch of elastic constants and thermal expansion coefficients of two member materials.

From this comparative study, it was found that the tungsten-to-metal joints showed the most severe stress evolution: the interfacial stress component normal to the interface was highly concentrated in the singular region in tensile direction. In contrast, the carbon based armour materials showed compressive stress with relatively mild intensification. The implication of the individual theoretical parameters and the limitation of their applicability as design factors were discussed.

References

[1] S. Timoshenko, J. Opt. Soc. Am. 11 (1925) 233.
[2] J.H. You, H. Bolt, R. Duwe, J. Linke, H. Nickel, J. Nucl. Mater. 250 (1997) 184.
[3] J.H. You, J. Mater. Eng. Perform. 7 (1998) 114.
[4] J.H. You, H. Bolt, this issue, p. 9.
[5] J.H. You, G. Breitbach, Fus. Eng. Des. 38 (1998) 307.
[6] K. Kitamura, K. Nagata, M. Shibui, N. Tachikawa, M. Araki, J. Nucl. Mater. 258–263 (1998) 275.
[7] K. Mizuno, K. Miyazawa, T. Suga, J. Faculty Eng., University of Tokyo (B) 39 (1988) 401.
[8] J.P. Blancard, N.M. Ghoniem, Trans. ASME J. Appl. Mech. 56 (1989) 756.
[9] D. Munz, Y.Y. Yang, Trans. ASME J. Appl. Mech. 59 (1992) 857.
[10] D. Post, J.D. Wood, B. Han, V.J. Parks, F.P. Gerstle Jr., Trans. ASME J. Appl. Mech. 61 (1994) 192.
[11] D.B. Bogy, Trans. ASME J. Appl. Mech. 38 (1971) 377.
[12] D. Munz, Y.Y. Yang, J. Eur. Ceram. Soc. 13 (1994) 453.
[13] F. Kroupa, Z. Knesel, J. Zemankova, in: M. Haviar (Ed.), Proceedings of the International Conference on Engineering Ceramic, Smolnice Castle, '92, 1992, p. 102.
[14] M. Fränkle, D. Munz, Y.Y. Yang, Int. J. Solids Struct. 33 (1996) 2039.
[15] J.H. You, Y.Y. Yang, Fus. Eng. Des. 38 (1998) 331.
[16] W. Delle, J. Linke, H. Nickel, E. Wallura, KFA Jülich, Report Jül-Spez-401, 1987.
[17] I. Smid, M. Akiba, M. Araki, S. Suzuki, K. Satoh, Japan Atomic Energy Research Institute, Report, JAERI-M 93–149, 1993.
[18] ITER Material properties handbook, ITER Document No. S74RE1 1997.
[19] A.F. Tavassoli, J. Nucl. Mater. 258–263 (1998) 85.
[20] J.H. You, Fus. Eng. Des. 38 (1998) 295.
[21] J.P. Blancard, N.M. Ghoniem, J. Nucl. Mater. 172 (1990) 54.